

Cite this: *Soft Matter*, 2012, **8**, 741

www.rsc.org/softmatter

PAPER

Characterization of a Ca binding-amphipathic silk-like protein and peptide with the sequence $(\text{Glu})_8(\text{Ala-Gly-Ser-Gly-Ala-Gly})_4$ with potential for bone repair

Aya Nagano,^a Hirohiko Sato,^b Yumi Tanioka,^c Yasumoto Nakazawa,^c David Knight^d and Tetsuo Asakura^{*c}

Received 29th August 2011, Accepted 11th October 2011

DOI: 10.1039/c1sm06646c

Bombyx mori silk fibroin with the main sequence $(\text{Ala-Gly-Ser-Gly-Ala-Gly})_n$ is a promising scaffold for bone regeneration not only on account of its excellent mechanical property as a structural matrix, but also for its slow biodegradability with adequate control of hydroxyapatite (HAP) deposition. Seeking to develop a material that might stimulate bone regeneration, we prepared a recombinant calcium binding-amphipathic silk-like protein $[(\text{Glu})_8(\text{Ala-Gly-Ser-Gly-Ala-Gly})_4]_4$ by expression in *E. coli*. We also prepared the homologous peptide $(\text{Glu})_8(\text{Ala-Gly-Ser-Gly-Ala-Gly})_4$ by solid phase synthesis. The poly-L-glutamic acid was introduced into both protein and peptide because this sequence is involved in HAP-nucleating domains of bone sialoprotein. The recombinant protein was shown to bind relatively large quantities of Ca^{2+} ions in solution by a spectrophotometric assay and in the solid state by X-ray photoelectron spectroscopy. Changes in the electronic structure and local conformation of the peptide resulting from Ca^{2+} binding were studied using ^{13}C solution NMR, especially ^{13}C chemical shifts. We obtained evidence that Ca^{2+} bound to the poly-L-glutamic acid domains but not to the predominantly hydrophobic $(\text{Ala-Gly-Ser-Gly-Ala-Gly})_4$ domains. A remarkable conformational change induced by adsorption of the synthetic peptide on the HAP surface was also demonstrated using ^{13}C solid state NMR.

Introduction

There is currently considerable interest in orthopedics for implantable materials that facilitate bone regeneration to substitute for autologous bone grafts.^{1–3} These materials should be biocompatible, osteogenic, resorbable, and capable of acting as a durable matrix that enhances the inward migration and/or delivery of cell populations, morphogens, and cytokines until newly formed host tissues can maintain these functions independently. Some protein-based biomaterials, such as collagen, have been examined in this capacity, but they lack the necessary mechanical properties. In contrast, silk-based materials offer superior mechanical properties that can be tailored to the application. In addition they degrade slowly compared with collagen, allowing load bearing throughout the bone remodeling process.^{4,5} Several previous studies have demonstrated the usefulness of silk fibroin-based porous scaffolds, many of which

facilitate bone repair by providing support for bone marrow stem cells or osteoblast-like cells.^{5–7} Thus, silk fibroin is a promising scaffold for bone regeneration not only because of its excellent mechanical property as a structural matrix, but also for its slow biodegradability and influence on hydroxyapatite (HAP) deposition.

The mineralization process is naturally induced in native bone by self-assembly at the charged acidic domains of non-collagenous proteins, which provide adequate conditions for nucleation of calcium HAP and development of ordered HAP crystals.^{8–12} These activities can also be mimicked *in vitro* by synthetic homopolymers or proteins containing poly-L-glutamic acids, $(\text{Glu})_n$, because $(\text{Glu})_n$ is involved in the HAP nucleating domains of bone sialoprotein. Thus, a new strategy for bone might use domains derived from a combination of the repeated sequence of AGSGAG in *B. mori* silk fibroin and the Ca-binding $(\text{Glu})_n$ domain.

In our previous paper,¹³ we reported the structural characterization of a family of silk-based water-soluble peptides, $(\text{Glu})_n(\text{Ala-Gly-Ser-Gly-Ala-Gly})_4 [(\text{E})_n(\text{AGSGAG})_4]$ where $n = 4–8$, using ^{13}C solid-state NMR. In these peptides, the sequence $(\text{AGSGAG})_4$ is markedly hydrophobic, while hydrophilic $(\text{E})_n$ not found in native silks is used to make the peptides water soluble when n is large enough. The effect on the local conformation of changing the balance of hydrophilic and hydrophobic

^aResearch and Technology Planning Office, Japan Medical Materials Corporation, Osaka, 532-0003, Japan

^bAnalysis Research Department, Chemical Laboratories, Nissan Chemical Industries LTD, Funabashi, Chiba, 274-8507, Japan

^cDepartment of Biotechnology, Tokyo University of Agriculture and Technology, Koganei, Tokyo, 184-8588, Japan. E-mail: asakura@cc.tuat.ac.jp

^dOxford Biomaterials Ltd, Magdalen Centre, Oxford, OX4 4GA, UK

domains by varying the number n in the $(E)_n$ in these peptides was studied using ^{13}C solid state NMR. When $n = 4$ and 5 , the conformation of the hydrophobic sequence was essentially silk I (the structure of *B. mori* silk fibroin in the silk gland before it is spun into a fiber) while the sequence $(E)_n$ was random coil. However, when $n = 6-8$ the structure of $(E)_n$ changed progressively from random coil to β -sheet, and the hydrophobic sequence took a mixture of β -sheet and random coil/distorted β -turn conformations, the fraction of the β -sheet conformation increasing with the increase in n from 6 to 8.

In this study, with the aim of developing new silk-based materials with potential for bone repair, we concentrated on the sequence $(E)_8(\text{AGSGAG})_4$. Here $(E)_n$ ($n = 8$) was selected because the peptide $(E)_8(\text{AGSGAG})_4$ was water soluble and the conformation of $(E)_8$ domain was mainly β -sheet in the solid state. We also report the synthesis of the recombinant silk-like protein, $[(E)_8(\text{AGSGAG})_4]_4$, using expression in *E. coli* as used^{20,21} for other recombinant silk-like proteins.^{14,15} The Ca^{2+} -binding activity of the protein was examined by a spectrophotometric method in solution and by X-ray photoelectron spectroscopy (XPS) in the solid state. Change in the electronic structure and in local conformation of the peptide $(E)_8(\text{AGSGAG})_4$ by Ca^{2+} binding was studied using ^{13}C solution NMR. The ^{13}C chemical shifts are sensitive to these changes. Therefore our attention will be focused on changes in the ^{13}C solution NMR chemical shift by Ca^{2+} binding.^{16,17,20} In addition, the conformational change of the peptide adsorbed on the HA surface was studied by ^{13}C CP/MAS NMR.

Materials and methods

Production of silk-like protein $[(E)_8(\text{AGSGAG})_4]_4$ by *E. coli*

The recombinant silk-like protein, $[(\text{AGSGAG})_4(E)_8\text{AS}]_4$, was prepared according to the method described previously^{14,15} in which the unit AS was included to allow polymerization by head-to-tail ligation. The oligonucleotide fragments encoding the crystalline region of *B. mori* silk fibroin and poly(L-glutamic acid) were ligated into pUC118 (Takara Bio. Inc. Japan) to construct a pUC118-linker vector containing a monomer providing SpeI and NheI restriction enzyme (Takara Bio. Inc., Japan) sites for the polymerization of target DNA (Fig. 1). Multimers of the sequence $(\text{AGSGAG})_4(E)_8\text{AS}$ were obtained by repeating the head-to-tail ligation and orientation for NheI and SpeI. After digestion of the recombinant monomer-containing pUC118, the fragment was ligated into the NheI–SpeI site of the

pUC118-linker. To construct the multimers, a pUC118-linker containing the monomer (or multimers) was digested with NheI to generate a linear vector containing the insert. Another insert-containing plasmid was digested with NheI and SpeI, liberating the inserted DNA fragment. Linearized vectors and inserted DNA fragments were extracted and ligated again. This process was repeated three times to polymerize the DNA sequence.

For the expression, digestion with BamHI and HindIII was used to excise multimerized DNA fragments from the pUC118-tetramer expression vector pET30a (Novagen, Germany). Protein expression was induced at $25\text{ }^\circ\text{C}$ by addition of isopropyl β -D-1 thiogalactopyranoside (IPTG) to a final concentration of 1 mM. The recombinant protein was purified by nickel-chelate chromatography using an ÄKTAexplorer 10S/100 (GE Healthcare, Waukesha, WI, USA) column. SDS–PAGE and western blotting were used to identify the expression. Its correct expression was confirmed by matrix-assisted laser desorption/ionization/time-of-flight mass spectrometry (MALDI/TOF-MS) (Voyager-DE PRO, Applied Biosystems, Foster City, CA, USA), the M_w peak at 19.9 kDa (theoretical M_w 19.7 kDa) indicating that the intended protein had been obtained.

Observation of Ca^{2+} binding activity of the recombinant silk-like protein

The reagents were purchased from WAKO (Shiga, Japan) or KANTO (Tokyo, Japan).

The Ca^{2+} -binding activity of the recombinant silk-like protein in aqueous solution was followed using a modification of previous spectrophotometric methods.^{18,19} For each run, a mixture of 1.5 mL of freshly prepared 100 mM NaHCO_3 (pH 8.7) and 300 μL of a solution containing 0, 0.125, 0.25, and 1.5 mg mL^{-1} of the silk-like protein made up in freshly prepared deionised water was placed in a cuvette with a 10 mm light path. 1.5 mL of 100 mM CaCl_2 solution was added at time zero with rapid mixing and the formation of a fine dispersion of insoluble CaCO_3 particles in the cuvette was monitored continuously at 570 nm in a V-530 type UV-vis spectrometer (JASCO Co., Tokyo, Japan) for 400 s by which time the absorption became practically asymptotic. The binding of Ca^{2+} ions to the silk-like protein has an inhibitory effect seen as a concentration-dependent decrease in the absorption at 570 nm at 400 s. The small quantities of silk-like protein that we could conveniently produce by expression precluded replication of this binding study but our previous work with this method for demonstrating calcium binding shows that it is reliable. However, calcium phosphate

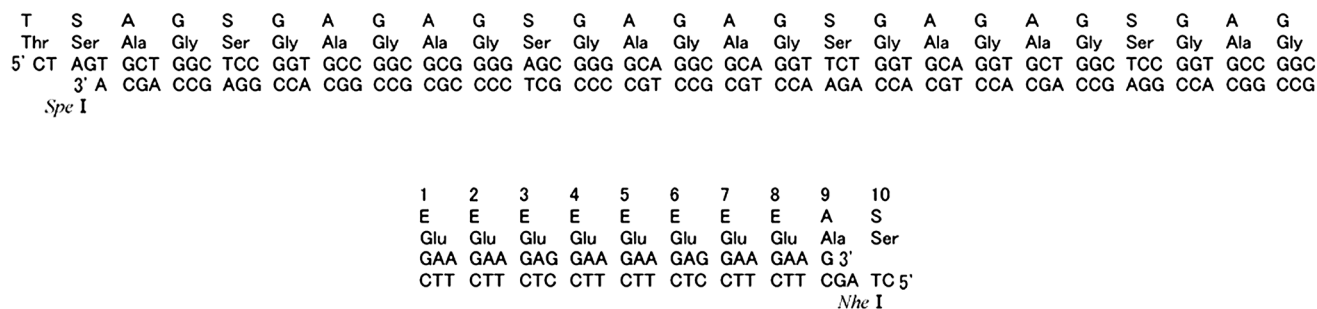


Fig. 1 Oligonucleotide sequences for the recombinant silk-like protein, $[(\text{AGSGAG})_4(E)_8\text{AS}]_4$.

precipitation can sometimes be induced non-specifically by biological materials in the absence of calcium binding so it was also necessary to confirm directly that the silk-like protein is capable of binding Ca^{2+} ions. This was done by X-ray photoelectron spectroscopy (XPS). For this, 20 μL of the aqueous solution of the silk-like protein was dropped on a PVDF membrane (Biorad, Tokyo, Japan), and the membrane was immersed in 1 mg mL^{-1} CaCl_2 solution and then rinsed three times in 50% v/v aqueous ethanol. The surface of the membrane was observed using XPS ESCA 5400 (ULVAC PHI, Tokyo, Japan) with a $\text{MgK}\alpha$ source. The XPS images were recorded at a 45° takeoff angle for the photoelectrons. The pass energy was 71.55 eV for narrow mode observation. The experiment was also performed on native silk fibroin under the same experimental conditions for comparison. The observations by XPS were repeated five times and the experimental error was calculated. The reproducibility of the data was confirmed.

^{13}C solution NMR observation of Ca^{2+} binding to the peptide $(\text{E})_8(\text{AGSGAG})_4$

Evidence for Ca^{2+} -binding to the silk-like protein in aqueous solution can be obtained directly by ^{13}C solution NMR. However, the protein at the concentration required for this technique is precipitated by the addition of calcium ions.²⁰ So instead we used the peptide with the sequence, $(\text{E})_8(\text{AGSGAG})_4$, which is not precipitated under the same conditions. This peptide was prepared by solid phase synthesis. The ^{13}C solution NMR spectra of the peptide were measured using a JEOL ECA-700 NMR spectrometer operating at 175 MHz. A total of 25–35 K scans were collected into 32 K data points using a delay time of 2 s. A stock solution of 210 mM CaCl_2 in 90% $\text{H}_2\text{O}/10\%$ D_2O solution was prepared for Ca^{2+} titration experiments. Approximately 4 mg of non-labeled $(\text{E})_8(\text{AGSGAG})_4$ was dissolved in 0.2 mL of 90% $\text{H}_2\text{O}/10\%$ D_2O solution. This solution was titrated by adding 5 μL aliquots of the stock CaCl_2 solution in four steps up to a total addition of 20 μL , collecting NMR spectra after each addition.

Adsorption of the peptide $(\text{E})_8(\text{AGSGAG})_4$ on the surface of hydroxyapatite particles

We used $(\text{E})_8(\text{AGSGAG})_4$ adsorbed on HAP particles (Sangi, Japan) as a model to study how the secondary structure of the silk-like protein might change when mineralized with HAP *in vitro* before implantation or when implanted into bone without prior mineralization. A suspension of 7 mL of 100 mg HAP particles (average particle size 3.3 μm) in deionized water was mixed with 1 mL of an aqueous solution (10 w/v%) of $(\text{E})_8(\text{AGSGAG})_4$, giving a final pH of 5.5. The resulting suspension was gently stirred for 3 days at room temperature. After centrifugation (15 000 rpm, 10 min, 4 $^\circ\text{C}$), the particles were washed 4 times with deionized water (pH 5.5) to remove the non-adsorbed peptide. The HAP particles were then dried *in vacuo*. The ^{13}C CP/MAS NMR spectrum of the peptide adsorbed on HAP particles was obtained on a Bruker DSX-400 AVANCE spectrometer with an operating frequency of 100.0 MHz for ^{13}C at a sample spinning rate of 8 kHz in a 4 mm diameter ZrO_2 rotor. The spectral width was 35 kHz with a recycle delay of 5 s and cross-polarization time was 2 ms under broad-band proton

decoupling. Phase cycling was used to minimize artifacts. 17 K scans were used for the peptide itself and 48 K scans were required for the peptide adsorbed on HAP. ^{13}C chemical shifts were calibrated indirectly using the adamantane methine peak relative to TMS (tetramethylsilane) at 0 ppm.

Results

Ca^{2+} binding activity of recombinant silk-like protein, $[(\text{AGSGAG})_4(\text{E})_8\text{AS}]_4$

Fig. 2 shows the effect of different initial concentrations of $[(\text{AGSGAG})_4(\text{E})_8\text{AS}]_4$ on the formation of CaCO_3 in a standard solution containing CaCl_2 and NaHCO_3 monitored continuously at 570 nm. The observed dose-dependent reduction in the absorption at 570 nm after 400 s indicates that the silk like protein $[(\text{AGSGAG})_4(\text{E})_8\text{AS}]_4$ binds calcium ions under the conditions used here.

Fig. 3 shows XPS of (a) the native silk fibroin and (b) the silk-like protein both adsorbed on the surface of membrane with (solid line) and without (broken line) immersion in CaCl_2 solution. The black trace in Fig. 3b shows two broad peaks, Ca 2p 3/2 (326.7 eV) and Ca 2p 1/2 (350.0 eV), demonstrating that it binds a relatively large mass of Ca^{2+} ions. The XPS observations were repeated five times; the average of c s^{-1} of the Ca 2p 3/2 peak was 4951 (standard deviation ± 52) and that of Ca 2p 1/2 was 3753 (SD ± 33). The two calcium peaks are just detectable in the native silk fibroin treated with CaCl_2 solution (solid line in Fig. 3a). Thus comparing Fig. 3a and b strongly suggests that the introduction of the poly(glutamic acid) component in the silk-like peptide $[(\text{AGSGAG})_4(\text{E})_8\text{AS}]_4$ greatly enhances its calcium binding relative to the native silk fibroin.

Ca^{2+} binding of the peptide $(\text{E})_8(\text{AGSGAG})_4$ monitored by ^{13}C solution NMR

Fig. 4a shows the ^{13}C solution NMR spectrum of the peptide $(\text{E})_8(\text{AGSGAG})_4$. The ^{13}C chemical shifts of main peaks are the

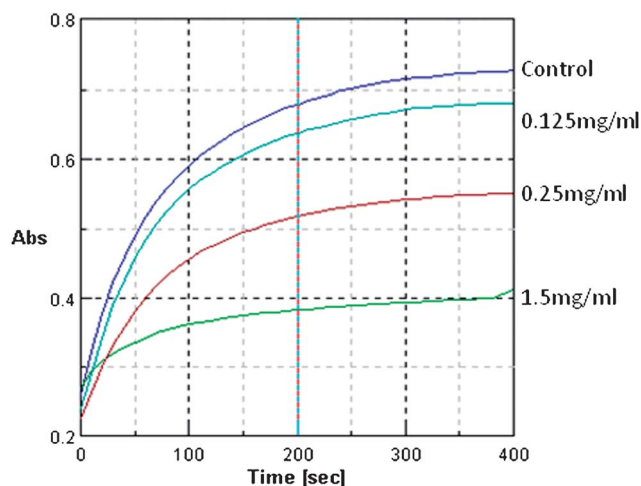


Fig. 2 Spectrophotometric evidence for Ca^{2+} -binding to the recombinant silk-like protein, by monitoring the effect of different concentrations of $[(\text{AGSGAG})_4(\text{E})_8\text{AS}]_4$ on formation of insoluble calcium carbonate in a solution containing NaHCO_3 and CaCl_2 (see text).

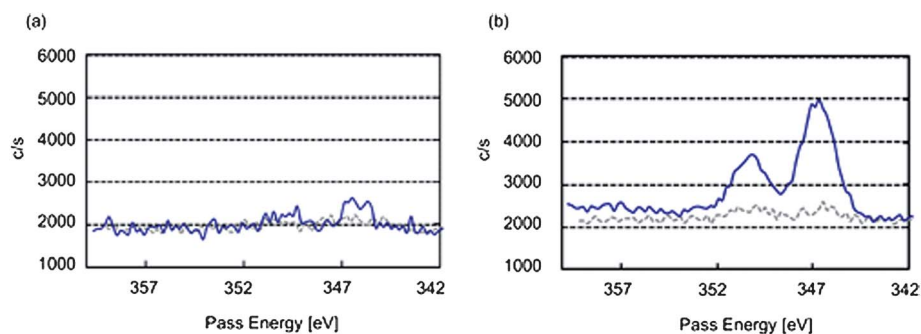


Fig. 3 XPS spectra showing the calcium content of (a) native silk fibroin and (b) recombinant silk-like protein before (broken line) and after (solid line) treatment with a solution containing Ca^{2+} ions.

same as those of the recombinant silk-like protein, indicating that the solution conformation is the same in both (data not shown). Therefore here we concentrate on the solution structure of the peptide $(\text{E})_8(\text{AGSGAG})_4$ instead of the protein. The main peaks observed at 16.7 ppm and 50.2 ppm were assigned respectively to the $\text{C}\beta$ and $\text{C}\alpha$ carbons of Ala residues indicating

that the region of the sequence $(\text{AGSGAG})_4$ takes random coil conformation in the aqueous solution.²⁰ This is supported by the chemical shifts of main peaks of Gly $\text{C}\alpha$, Ser $\text{C}\alpha$ and Ser $\text{C}\beta$ carbons observed at 42.9 ppm, 56.1 ppm and 61.5 ppm respectively. The carbonyl region yielded detailed information on the conformation at different residues in the crystalline regions of *B*.

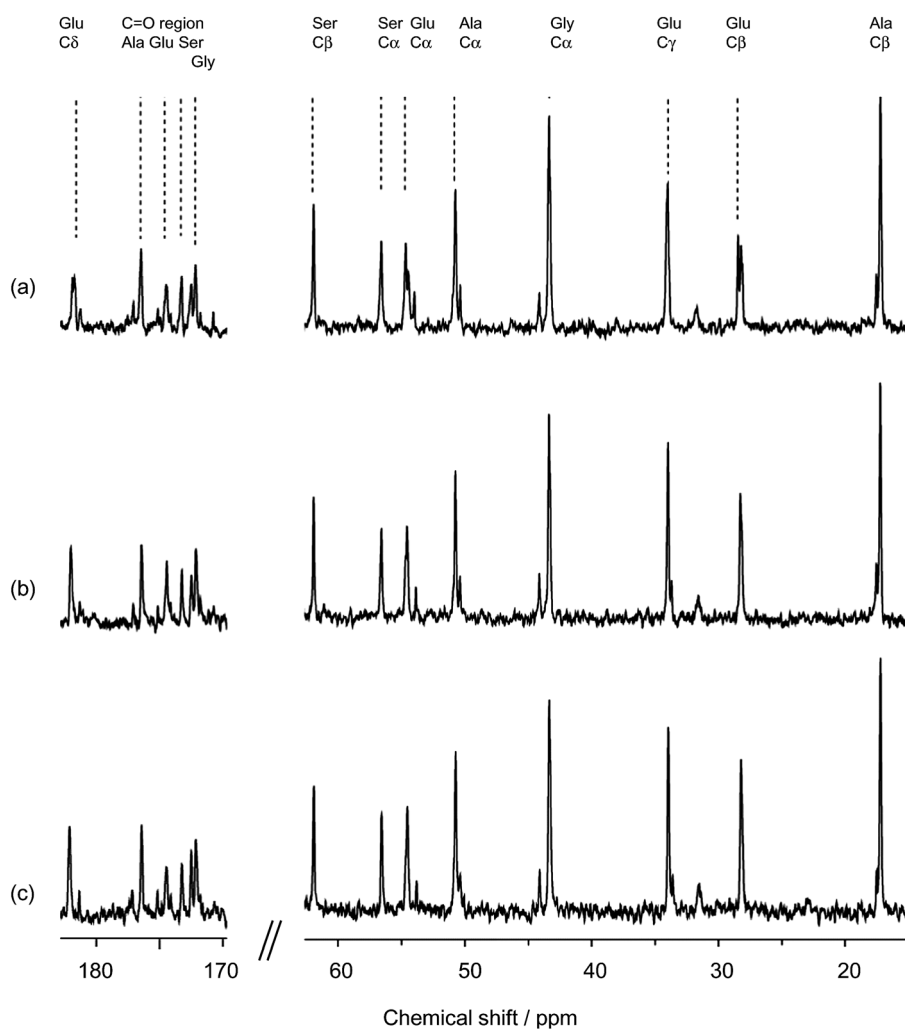


Fig. 4 The effect of different concentrations of Ca^{2+} ions on the ^{13}C solution NMR spectra of $(\text{E})_8(\text{AGSGAG})_4$. The assignments are also shown. (a) No added Ca^{2+} ions; (b) solution with a peptide/ CaCl_2 molar ratio of 1 : 4, and (c) solution with a peptide/ CaCl_2 molar ratio of 1 : 9 (see text).

mori.²¹ In accordance with these data, in the present study we assign the main peaks in the carbonyl region for (E)₈(AGSGAG)₄ to the carbonyl carbons of GAG (175.97 ppm), GSG (172.75 ppm), AGS (172.00 ppm) and AGA (171.68 ppm) which have essentially the same chemical shifts as the corresponding ones in *B. mori* silk fibroin in aqueous solution. The small peaks observed around the main peaks of Gly and Ala residues which correspond to one residue judged by their relative intensities can be assigned to the Ala-Gly (*C*-terminal) residue in the peptide.

Turning to the (E)₈ region of the peptide, except for the C γ peak the peaks from the carbons of the Glu residue are separated slightly and have the following chemical shifts: 53.5 ppm, 54.0 ppm and 54.2 ppm for Glu C α carbon; 27.6 ppm, 27.7 ppm and 28.0 ppm for Glu C β carbon; and 33.5 ppm for Glu C γ carbons. However, the range of the chemical shift distribution is not large and can be assigned to random coil conformation for which shifts of 54.5 ppm for Glu C α carbon, 27.7 ppm for Glu C β carbon and 33.8 ppm for Glu C γ carbons have been measured in a previous study.²² The small peak such as 53.5 ppm for the Glu C α carbon can be assigned to the *N*-terminal E in the peptide. Thus, the local conformation of both the hydrophilic region (E)₈ and the predominantly hydrophobic region (AGSGAG)₄ seems to be in random coil conformation.

A possible change in the electronic structure and local conformation of the peptide, (E)₈(AGSGAG)₄, induced by Ca²⁺ binding was studied using ¹³C solution NMR. Fig. 4a–c show that there were no changes in the ¹³C solution NMR spectra of the hydrophobic region (AGSGAG)₄ of the peptide caused by the addition of Ca²⁺ ions to the aqueous solution [molar ratios of peptide/CaCl₂ = 1/4 (Fig. 4b) and 1/9 (Fig. 4c)]. This confirms that Ca²⁺ ions do not bind to this hydrophobic region. In contrast, there are significant changes in the ¹³C solution NMR spectra of the hydrophilic region (E)₈ on addition of Ca²⁺ ions. Tomlinson *et al.* reported the pH-dependent changes in the NMR solution chemical shifts of amide protons, amide nitrogens

and carbonyl carbons of glutamic acid residues in the *Staphylococcal* protein G B1 domain (GB1).²³ These large pH-dependent chemical shift changes were observed by titrating side chains. Thus to be sure that the chemical shifts we observed were produced by changes in Ca²⁺ concentration rather than by accidental changes in pH on adding Ca²⁺, we checked the pH of the peptide solution before and after adding calcium ions and obtained pH values of 6.1 for the peptide only and 6.1 and 6.2 respectively for the peptide/CaCl₂ solution with molar ratios of 1 : 4 and 1 : 9. This strongly indicates that the change in the chemical shifts in this work is indeed due to Ca²⁺ binding.

The expanded ¹³C NMR spectra of the glutamic acid residues are shown in Fig. 5. The lower field shift of the main peak of the Glu C δ carbon and high field shift of the Glu C γ carbon with alternative shifts reflect the polarization effect of the C(δ)–C(γ) bond induced by Ca²⁺ binding. As the extent of Ca²⁺ binding increased, the size of both the lower field shift of C δ and of the high field shift of C γ should increase. The extent of this affect varied at each Glu residue peak, implying that the degree of the Ca²⁺ binding is different depending on the position of the Glu residue in the peptide although the assignment of each peak in the carbons is difficult. The polarization effect should in theory be smaller for Glu C β and Glu C α carbons due to the long distance from the Ca²⁺ binding site, that is, the C(δ) O₂[−] group. However, significant chemical shift changes were also observed for both these carbons. This indicates that Ca²⁺ binding induces a conformational change in the backbone of the (E)₈ chains.²⁰

¹³C CP/MAS NMR spectra of the peptide E₈(AGSGAG)₄ absorbed on hydroxyapatite

Next, we consider the effect on the secondary structure of the peptide, (E)₈(AGSGAG)₄, of adsorption onto HAP as determined by ¹³C CP/MAS NMR. Fig. 6 shows a comparison of the ¹³C CP/MAS NMR spectra of (E)₈(AGSGAG)₄ (a) before and

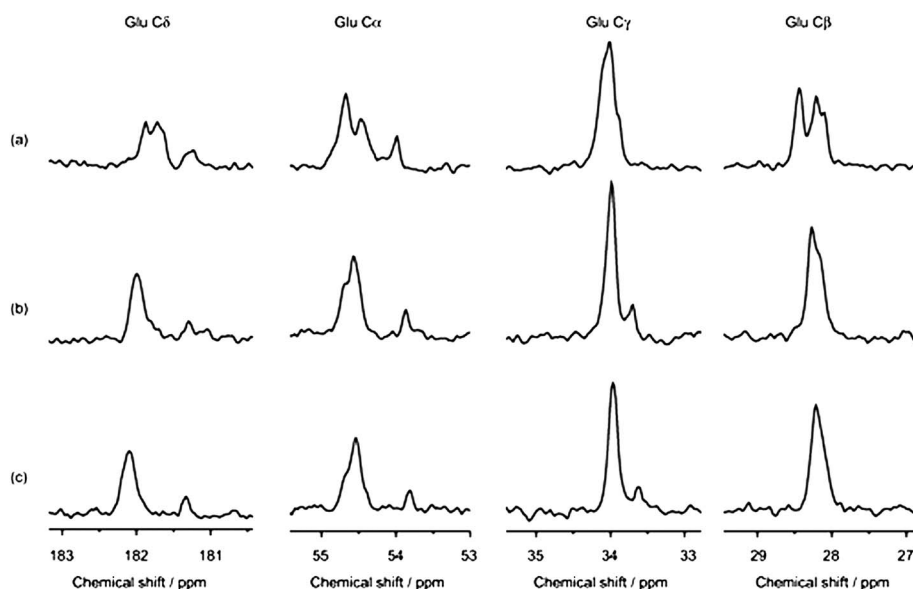


Fig. 5 The expanded ¹³C solution NMR spectra of individual carbons in the (E)₈ sequence in (E)₈(AGSGAG)₄. (a) No added Ca²⁺ ions; (b) solution with a peptide/CaCl₂ molar ratio of 1 : 4, and (c) solution with a peptide/CaCl₂ molar ratio of 1 : 9.

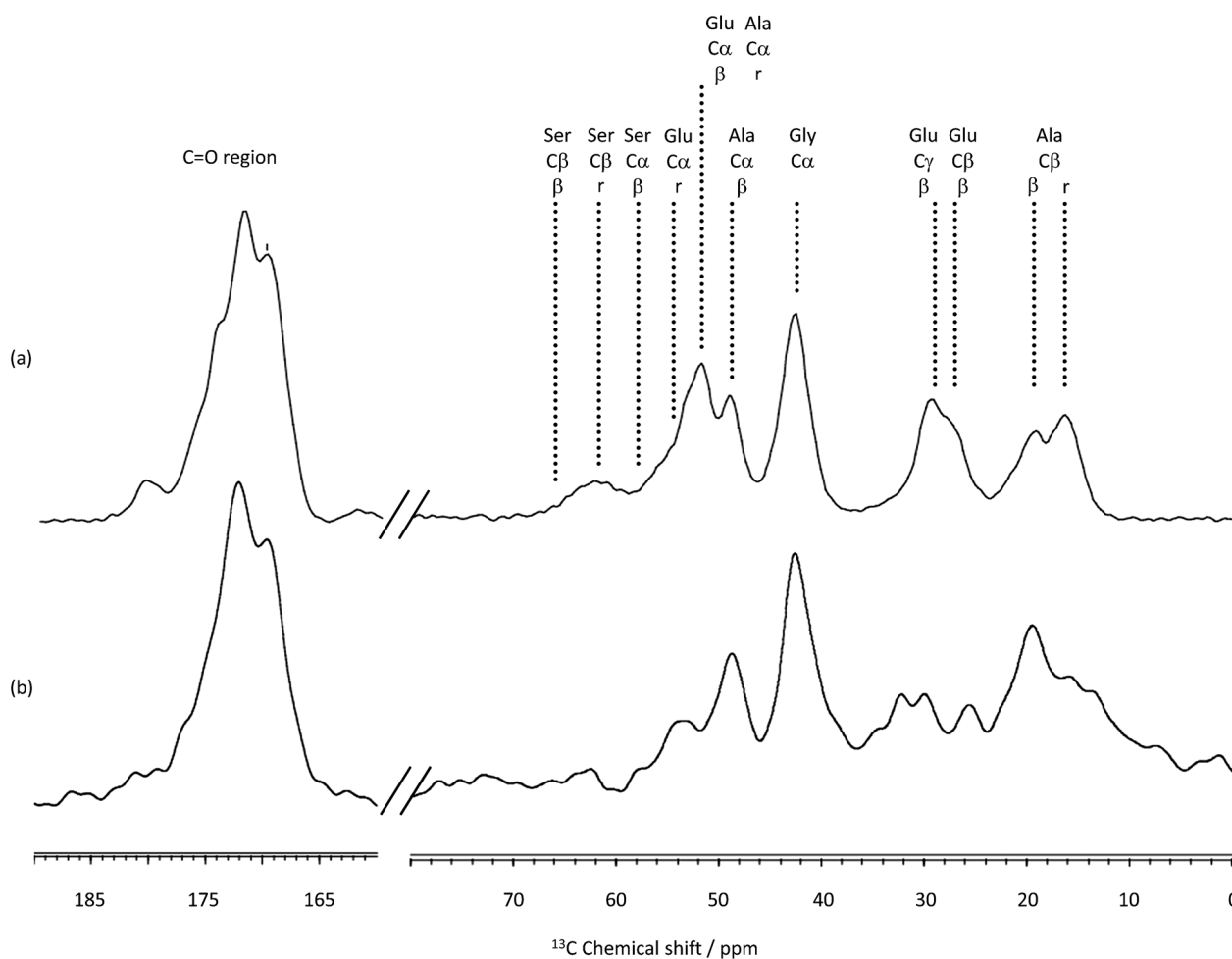


Fig. 6 ^{13}C CP/MAS NMR spectra of $(\text{E})_8(\text{AGSGAG})_4$ (a) before and (b) after adsorption on HAP particles. “r” and “ β ” mean random coil and β -sheet structure, respectively.

(b) after adsorption on HAP particles. The S/N ratio of the spectrum (b) is very low as a result of the very small quantity of peptide adsorbed on the particles. The spectrum (a) before adsorption is essentially the same as the spectrum reported previously.¹³ Only the $(\text{E})_8$ domain is slightly different; comparing Fig. 5 with the spectrum presented in the previous paper,¹³ we see differences in the chemical shifts for both $\text{C}\beta$ and $\text{C}\gamma$ carbons although a $\text{C}\beta$ shift is observed as a shoulder of the $\text{C}\gamma$ peak. This is thought to be due to a small difference in pH of the solution during the drying of the solid samples in the previous and present paper. The $\text{Gly C}\alpha$ peak is not sensitive to the conformation but Ala and Ser carbon peaks are sensitive. For example, the peaks observed at 20 ppm and 17 ppm in Fig. 6a are assigned to the β -sheet and the random coil of the Ala residue respectively^{24–26} and the fraction of random coil is slightly larger judging from the relative intensities. In addition, the relatively sharp peaks with a shoulder observed at 52 ppm and 30 ppm assigned to $\text{Glu C}\alpha$ and $\text{Glu C}\beta$ carbons, respectively, indicate that the structure of the $(\text{E})_8$ region is mainly β -sheet.¹³

The structure of $(\text{E})_8(\text{AGSGAG})_4$ is largely changed on adsorption onto HAP particles. Although the S/N ratio of the ^{13}C CP/MAS NMR is low, the increase of the peak intensities of the Ala $\text{C}\beta$ peak clearly indicates that the amounts of β -sheet

structure increased by binding to HAP. This is supported by the increase in the Ala $\text{C}\alpha$ β -sheet peak. With regard to changes in $(\text{E})_8$ domain, the peaks become considerably broader in the $\text{Glu C}\alpha$ and $\text{Glu C}\beta$ carbons after adsorption to HAP expanding to lie between 24 and 32 ppm. Unfortunately the low S/N ratio makes it difficult to assign each peak in this region. The $\text{Glu C}\alpha$ peak is also broadened by HAP binding. Thus, the binding of the carboxyl side chains of the $(\text{E})_8$ region to the calcium atoms on the surface of HAP particles influences the structure of this domain though the details of this conformation change are yet to be determined.

Discussion

It has been suggested that acidic sites regulate mineral formation in non-collagenous proteins such as bone sialoprotein (BSP), osteopontin (OPN), and osteocalcin (OCN).^{8,27–31} However, it is not yet clear whether HAP nucleation is affected more by the number of acidic sites or by the protein conformation. Harris *et al.* showed that recombinant peptides derived from porcine BSP residues 42–87 containing $(\text{E})_n$ sites ($n = 1, 2, 3$ and 8) and poly(glutamic acid) as a positive control had nucleating activity, while peptide residues 69–300 containing $(\text{E})_n$ sites ($n = 1, 2, 3$

and 6) lack activity.⁸ In their similar experiment,⁸ recombinant peptide derived from porcine BSP residues 133–272 containing (E)_n sites ($n = 1, 2, 3$ and 6) had nucleating activity, while peptide residues 42–125 containing (E)_n sites ($n = 1, 2, 3$ and 8) lack activity. They suggested that the causal factors for these differences were the presence or absence of phosphorylation or differences in folding or conformation. Our results suggest that proteins have an optimal combination of characteristics for calcium-binding, including type and number and conformation of acidic amino acid sites. Previous studies suggest that for glutamic acid the threshold number of residues is $n = 6–8$. Thus the ability demonstrated in the present communication of (E)₈(AGSGAG)₄ to bind Ca²⁺ ions (Fig. 3a and b) is thought to depend in part on having sufficient acidic residues.

The high field shift of the Glu C α carbon induced by Ca²⁺-binding (Fig. 5b and c) suggests that the binding produces a partial conformational change from random coil to β -sheet structure. The amount of the shift is different in each peak of Glu C α and Glu C β , respectively, implying that both the affinity for Ca²⁺-binding and the extent of the conformational change depend on the position of the glutamic acid in the (E)₈ sequence.

Native bone tissue is composed of a complex matrix of collagen and non-collagenous proteins such as BSP, OPN and OCN.^{8,27–31} The mineralization process is naturally induced in bone by non-collagenous proteins with negatively charged acidic domains which provide adequate conditions for the nucleation and control of the size, orientation and epitaxial growth of HAP crystals during growth and remodelling. In non-collagenous bone proteins, negatively charged acidic domains such as (E)_{6–10} in BSP,^{8,29} poly(aspartic acid) domain (D)₉ and phosphorylated amino acids in OPN,¹² and γ -carboxyglutamic acid residues in OCN are implicated in HAP nucleation.^{27,28,31} Of particular significance, BSP has been reported to be localized in osteoid, the matrix ahead of the mineralization front in developing bone. Studies using a steady-state agarose/gelatin gel system have shown that BSP is a potent HAP nucleator.⁸ These activities can also be mimicked *in vitro* by synthetic homopolymers containing glutamic acid or proteins containing poly(glutamic acid).²⁹ Encouraged with these findings, we have focused on the introduction of poly(glutamic acid) as HAP nucleation sites in artificial proteins, designing a novel recombinant protein containing these domains required for solubility as well as mineralization. In addition our recombinant protein contains the predominantly hydrophobic sequence that forms much of the β -sheet crystalline regions of *B. mori* fibroin which in turn play an important role in the assembly and mechanical properties of the native silk fiber. Thus our recombinant protein and the analogous peptide are amphiphilic. These considerations suggest that it might be possible to design liquid crystalline proteins or other liquid crystalline synthetic constructs containing E_n(AGSGAG)_m that owe their liquid crystallinity to their amphiphilicity and net negative charge, and are therefore self-assembling, as well as calcium binding. The latter two properties would help to give them the ability to nucleate hydroxyapatite. Indeed, recent studies indicate that self-assembly of proteins plays a key role in natural mineralization processes.^{27,28} In this connection it is already known that in dentine matrix proteins in the bone-like tissue of the teeth, extensive phosphorylation of serine domains introduces acidic side chains. This domain acts as a Ca²⁺ binding

site with a β -sheet conformation, promoting HAP crystal development. Interestingly, the β -sheet conformation provides a planar surface where the distance between two serine residues is about the same as that between two Ca atoms of HAP.²⁸ This is thought to promote crystal nucleation.³¹ Further, dentine matrix protein 1 in the presence of Ca²⁺ self-assembles by forming intermolecular calcium ion bridges, to give aggregates that initiate apatite crystallization.³⁰ BSP non-collagenous proteins in bone exhibit similar characteristics that initiate and maintain HAP nucleation.³² In this case, the protein contains poly(glutamic acid) sites, also in a β -sheet conformation. To generalize, extracellular matrices responsible for biomineralization are based on proteins containing bioactive acidic motives and self-assemble, promoting HAP crystal growth.^{27,28,31} These considerations and the evidence presented above that (E)₈(AGSGAG)₄ acts as a Ca²⁺ binding site with β -sheet conformation suggest that in general poly(glutamic acid) sites in β -sheet conformation should promote HAP crystal formation.

Thus synthetic silk-like proteins containing poly(glutamic acid) or related constructs are good candidates in the search for advanced bone repair materials with potential applications in orthopaedics and maxillofacial surgery.

Conclusions

A recombinant calcium binding-amphiphilic silk-like protein with the sequence, [(Glu)₈(Ala-Gly-Ser-Gly-Ala-Gly)₄]₄, was expressed in *E. coli* and the peptide (Glu)₈(Ala-Gly-Ser-Gly-Ala-Gly)₄ was produced by solid state synthesis. Both constructs therefore contained the poly-L-glutamic acid involved in HAP-nucleating domains of bone sialoprotein and a mainly hydrophobic domain derived from the crystalline regions of *Bombyx mori* silk fibroin. Both constructs showed a high capacity for binding Ca²⁺ ions. Evidence that the conformation of the poly(glutamic acid) domains of the construct were altered by binding calcium ions or by interacting with the surface of hydroxyapatite particles was obtained respectively by solution and solid state NMR. Our observation suggests that this recombinant silk-like protein or constructs related to it may be candidates for use in bone repair.

Acknowledgements

T.A. acknowledges support by grant from the Ministry of Agriculture, Forestry and Fisheries of Japan (Agri-Health Translational Research Project) (2010–2015).

Notes and references

- 1 M. P. McAndrew, P. W. Gorman and T. A. Lange, *J. Orthop. Trauma*, 1988, **2**, 333–339.
- 2 J. O. Hollinger, J. Brekke, E. Gruskin and D. Lee, *Clin. Orthop. Relat. Res.*, 1996, **324**, 55–65.
- 3 J. Y. Reginster, *Rheumatology*, 2002, **41**, 3–6.
- 4 K. Makaya, S. Terada, K. Ohgo and T. Asakura, *J. Biosci. Bioeng.*, 2009, **108**, 68–75.
- 5 S. Hofmann, H. Hagenmüller, A. M. Koch, R. Müller, G. Vunjak-Novakovic, D. L. Kaplan, H. P. Merkle and L. Meinel, *Biomaterials*, 2007, **28**, 1152–1162.
- 6 H. J. Kim, U. J. Kim, H. S. Kim, C. Li, M. Wada, G. G. Leisk and D. L. Kaplan, *Bone*, 2008, **42**, 1226–1234.

-
- 7 L. Meinel, O. Betz, R. Fajardo, S. Hofmann, A. Nazarian, E. Cory, M. Hilbe, J. McCool, R. Langer and G. Vunjak-Novakovic, *Bone*, 2006, **39**, 922–931.
 - 8 N. L. Harris, K. R. Rattray, C. E. Tye, T. M. Underhill, M. J. Somerman, J. A. D'errico, A. F. Chambers, G. K. Hunter and H. A. Goldberg, *Bone*, 2000, **27**, 795–802.
 - 9 J. T. Stubbs Iii, K. P. Mintz, E. D. Eanes, D. A. Torchia and L. W. Fisher, *J. Bone Miner. Res.*, 1997, **12**, 1210–1222.
 - 10 B. Ganss, R. H. Kim and J. Sodek, *Crit. Rev. Oral Biol. Med.*, 1999, **10**, 79.
 - 11 H. I. Roach, *Cell Biol. Int.*, 1994, **18**, 617–628.
 - 12 A. L. Boskey, *Ann. N. Y. Acad. Sci.*, 1995, **760**, 249.
 - 13 A. Nagano, Y. Kikuchi, H. Sato, Y. Nakazawa and T. Asakura, *Macromolecules*, 2009, **42**, 8950–8958.
 - 14 M. Yang, T. Muto, D. Knight, A. M. Collins and T. Asakura, *Biomacromolecules*, 2008, **9**, 416–420.
 - 15 S. Yanagisawa, Z. Zhu, I. Kobayashi, K. Uchino, Y. Tamada, T. Tamura and T. Asakura, *Biomacromolecules*, 2007, **8**, 3487–3492.
 - 16 A. Cavalli, X. Salvatella, C. M. Dobson and M. Vendruscolo, *Proc. Natl. Acad. Sci. U. S. A.*, 2007, **104**, 9615–9620.
 - 17 S. Neal, A. M. Nip, H. Zhang and D. S. Wishart, *J. Biomol. NMR*, 2003, **26**, 215–240.
 - 18 H. Inoue, N. Ozaki and H. Nagasawa, *Biosci., Biotechnol., Biochem.*, 2001, **65**, 1840–1848.
 - 19 S. Hidaka, T. Matsuo and K. Ouchi, *J. Dent. Health*, 2003, **53**, 137–144.
 - 20 T. Asakura, Y. Watanabe, A. Uchida and H. Minagawa, *Macromolecules*, 1984, **17**, 1075–1081.
 - 21 T. Asakura, Y. Watanabe and T. Itoh, *Macromolecules*, 1984, **17**, 2421–2426.
 - 22 M. Iwadate, T. Asakura and M. P. Williamson, *J. Biomol. NMR*, 1999, **13**, 199–211.
 - 23 J. H. Tomlinson, V. L. Green, P. J. Baker and M. P. Williamson, *Proteins: Struct., Funct., Bioinf.*, 2010, **78**, 3000–3016.
 - 24 T. Asakura, H. Sato, F. Moro, M. Yang, Y. Nakazawa, A. M. Collins and D. Knight, *Macromolecules*, 2007, **40**, 8983–8990.
 - 25 T. Asakura, M. Hamada, S. W. Ha and D. P. Knight, *Biomacromolecules*, 2006, **7**, 1996–2002.
 - 26 T. Asakura, K. Nitta, M. Yang, J. Yao, Y. Nakazawa and D. L. Kaplan, *Biomacromolecules*, 2003, **4**, 815–820.
 - 27 Y. Meng, Y. X. Qin, E. DiMasi, X. Ba, M. Rafailovich and N. Pernodet, *Tissue Eng. A*, 2009, **15**, 355–366.
 - 28 C. E. Semino, *J. Dent. Res.*, 2008, **87**, 606–616.
 - 29 H. A. Goldberg, K. J. Warner, M. J. Stillman and G. K. Hunter, *Connect. Tissue Res.*, 1996, **35**, 385–392.
 - 30 G. He, T. Dahl, A. Veis and A. George, *Nat. Mater.*, 2003, **2**, 552–558.
 - 31 L. Addadi, S. Weiner and M. Geva, *Z. Kardiol.*, 2001, **90**, III92–98.
 - 32 C. E. Tye, K. R. Rattray, K. J. Warner, J. A. R. Gordon, J. Sodek, G. K. Hunter and H. A. Goldberg, *J. Biol. Chem.*, 2003, **278**, 7949.